

## Neural network-based estimation and compensation of friction for enhanced deep drawing process control

THIERY Sebastian<sup>1,a\*</sup>, EL ABDINE Mazhar Zein<sup>1,b</sup>, HEGER Jens<sup>1,c</sup> and BEN KHALIFA Noomane<sup>1,2,d</sup>

<sup>1</sup> Institute for Production Technology and Systems, Leuphana University Lüneburg, Universitätsallee 1, 21335 Lüneburg, Germany

<sup>2</sup> Institute of Material and Process Design, Helmholtz-Zentrum Hereon, Max-Planck-Str. 1, 21502 Geesthacht, Germany

<sup>a</sup>sebastian.thiery@leuphana.de, <sup>b</sup>mazhar.abdine@leuphana.de, <sup>c</sup>jens.heger@leuphana.de, <sup>d</sup>noomane.ben\_khalifa@leuphana.de

**Keywords:** Deep Drawing, Material Draw-In, Predictive Modelling, Friction Estimation, Closed-Loop Control, Process Monitoring and Stabilization, Particle Swarm Optimization

**Abstract.** Fluctuating process conditions, such as lubrication, can disturb the production process and lead to faulty components that have cracks or wrinkles. Real-time identification of process parameters can detect deviations in sheet forming operations and enable the process parameters to be adjusted. To increase process robustness, closed-loop control is often used to monitor and influence the material draw-in, which corresponds to the material flow and can be measured by camera systems inside the deep-drawing press. The aim of this work is to develop a control concept that can predict the optimum blank holder force by estimating the coefficient of friction based on the material draw-in of the last stroke. Using a cross-die geometry, it is shown how the material draw-in can be determined experimentally by means of a camera system and numerically by FE simulations. Finally, artificial neural network-based models are trained through simulations and are subsequently tested on a numerical case study in which the coefficient of friction is changed as a disturbance variable and must be compensated for. The widely applicable control concept has the potential to incorporate additional softsensors, for example to determine material properties, and other target variables, such as the punch force, into the optimization algorithm.

### Introduction

With increasing component complexity in the automotive industry, the sensitivity of deep drawing operations to process fluctuations increases, which leads to a narrowing of the process window. Due to the high cost pressure, press lines must develop efficient strategies to avoid the occurrence of defects under these challenging conditions. One solution to this is closed-loop control, in which quality-relevant product characteristics are monitored and, if necessary, appropriate actuators are used to make the necessary adjustments to the process parameters. Recently, various approaches were presented for recording component quality by means of optical measurements using camera systems installed in the press and integrating them into closed-loop controls. In addition, there is great potential in data-driven modeling to optimize the manufacturing process or for real-time identification of disturbances during deep drawing.

Deep drawing processes are non-static due to fluctuations, where disturbances can have a negative impact on process stability over time [1]. Short-term disturbances include, for example, variable sheet thickness. Varying material properties, tool wear and tool temperature are examples of long-term disturbances. To that end, the tool warms up at the start of a batch and influences the lubrication conditions as well as the friction behavior between the sheet metal and the tool [2]. Depending on the time characteristics of these disturbances, different concepts can be selected in

order to create a closed-loop control to compensate for them. Whereas offline controls are better suited for long-term disturbances, as they measure the component properties between two or more strokes and can make adjustments to the process parameters with a time delay [3], online controls are preferable for short-term disturbances, as they can adjust the process parameters during the stroke. Lo and Yang [4] proposed a concept to detect the minimum side wall thickness and the wrinkle height during the deep drawing process and to continuously adjust the blank holder force (BHF) over the drawing depth by a control algorithm. This concept shows that the choice of sensor technology is linked to the target variable of the control system. Siegert et al. [5] developed a sensor to measure the frictional force between blank and die. They successfully demonstrated that the BHF can be adjusted to achieve a constant frictional force despite varying amounts of lubricant. Force sensors can also be integrated into the punch, as the forming process can be characterized via the punch force [6]. In most cases, however, the material draw-in or material flow is measured to control the deep drawing process even in cases where accessibility of the workpiece in the tool is restricted. For example, Behrens et al. [7] developed a special optical sensor for a contact-free measurement of the material flow.

The potential of machine vision for contactless quality monitoring and component measurement is constantly increasing in deep drawing. One of the first examples of online defect detection in the press shop is the image acquisition system from Gayubo et al. [8], in which the components were inspected at the end of the press line by a camera operated by a robot. A valley detection algorithm was used to identify the cracks. Current developments show that convolutional autoencoders can also be used to detect faulty components, including wrinkles [9]. However, indirect quality features can be defined and visually evaluated instead of directly identifying the defects, such as the material draw-in after the first drawing stage [10]. This offers the advantage of possibly detecting interior cracks or ruptures, which would be otherwise challenging. Moreover, this increases the time-window where corresponding countermeasures can be adopted before the faulty part reaches the end of line inspection. In the case that the flange is cut off before the image can be captured, the material flow can alternatively be measured via the position of the skid-lines [11]. This strategy enables continuous quality monitoring, where intervention limits can be set for the position of the skid-lines, indicating when action is required to prevent part failure [12]. Additionally, camera-based quality monitoring offers advantages for press hardening [13]. Optical systems can also be used as sensors for closed-loop control. Using a kitchen sink as an example, Fisher et al. [14] demonstrated that the draw-in can be controlled using a proportional control algorithm to adjust the BHF. Various control algorithms can be used to stabilize the deep drawing process. A controller designed as an optimal control problem gives good results in the example of a front fender and has an integral behavior [15].

Machine learning methods, in particular employing artificial neural networks (ANNs), can be applied in the context of intelligent process control and process optimization. ANNs are suitable for training models which act as *softsensors*, estimating otherwise unmeasurable product properties and process parameters based on known data [16]. Zhao and Wang [17] trained an ANN for the determination of friction conditions on the basis of the punch force and other process parameters. In a similar way, varying material properties can be identified [18]. An alternative for measuring material properties is the eddy current based material testing, which can be integrated directly into the production process [19]. Mork [20] combined this non-destructive material testing with an ANN to make predictions about the quality of each component and, if necessary, automatically adjust the deep drawing process. Further, ANNs can be employed in combination with an optimization algorithm and aid in identifying the optimum parameters for deep drawing processes. Tai and Lin [21] applied a simulated annealing optimization algorithm to an ANN to search for the optimal clearance between punch and die. This strategy was also used to improve sheet thinning during deep drawing [22]. Particle Swarm Optimization (PSO), belonging to the

family of meta-heuristic optimization algorithms, is another example of a widely used algorithm. El Mrabti et al. [23] first used a finite element model to generate a database with which they trained an ANN to predict springback. The authors then applied PSO to determine the best settings for the BHF and punch speed to minimize springback.

In this study, a concept for estimating and compensating of friction for enhanced deep drawing process control is presented. First, a camera system is introduced to measure the draw-in during the experimental investigation of the deep drawing process. Next, a finite element model is developed to map the influence of the coefficient of friction on the draw-in. The control concept is then described, which includes a softsensor for estimating the coefficient of friction and a PSO-based optimization algorithm. This concept requires the training of two ANN-based regression models, one to estimate the coefficient of friction and, by extension, the lubrication condition and another for estimating the draw-in. Finally, the effectiveness of the control for stabilizing the deep drawing process is tested on a numerical case study.

### Experimental and numerical setup

Experiments and simulations are used to investigate the behavior of the draw-in with respect to press parameters, material properties and lubrication conditions. The experiments are carried out on a hydraulic press with a drawing cushion. A cross-die shape is selected as the geometry (Fig. 1a). Sensors to measure ram force and BHF are integrated into the press. A *SelVision* monitoring system provided by the metrology specialists Selmatic Systems GmbH was installed in the press to measure the draw-in. The installed system consists of two cameras mounted in opposite corners of the hydraulic press (Fig. 1b). An interface was consequently set up between the monitoring system and the press control system. This enables continuous recording of the process forces and the tool position for each stroke and their automatic mapping to the images taken by the cameras.

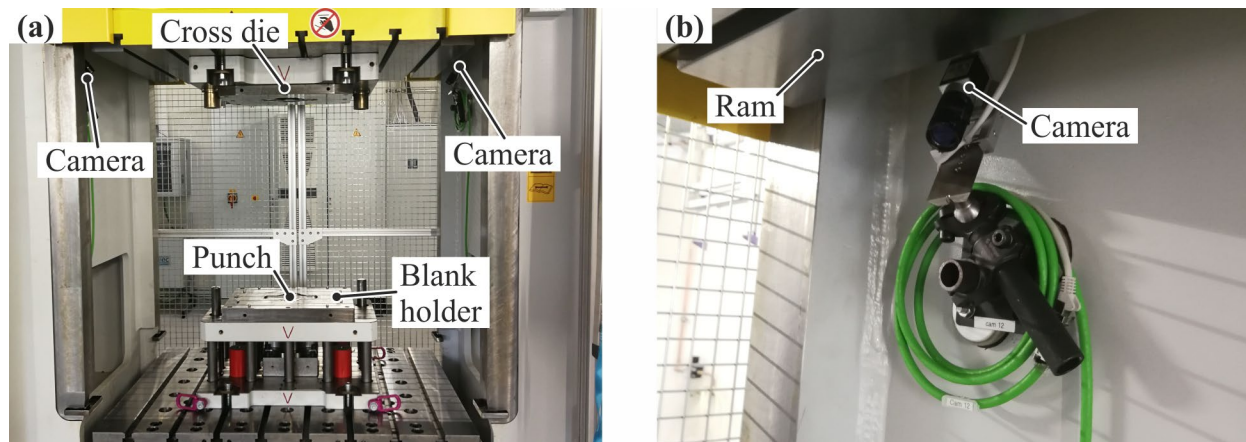


Fig. 1. (a) Cross-die tool in the hydraulic press and (b) close-up of the camera on the right side

Experiments with the parameters listed in Table 1 show that each parameter change has a considerable effect on the draw-in measured by the cameras. On the one hand, the viscosity of the lubricant affects the friction, with lower viscosities shortening the draw-in and provoking material cracks. On the other hand, the BHF also influences friction, with low BHF lengthening the draw-in. The BHF is therefore generally suitable for compensation for changes in lubrication conditions.

Table 1. Parameters for the deep drawing experiments

Parameter	Value
Material and thickness $t$ [mm]	DC04 (0.7 – 1.0); DC01 (0.8 – 1.0)
Blank holder force $F_{BH}$ [kN]	40 – 170 – 300 – 430 – 560 – 690
Drawing velocity $v$ [mm/s]	5 – 30
Lubricant viscosity $\eta$ [mm <sup>2</sup> /s]	100 – 400
Drawing depth $h$ [mm]	55

To test the measuring accuracy of the monitoring system, selected components were measured using an ATOS 3D-Scanner. Fig. 2a shows the results for the material DC04 with a thickness of 1 mm at a drawing speed of 30 mm/s using the lubricant with a viscosity of 100 mm<sup>2</sup>/s. The camera system automatically captures the greyscale images after each stroke when the blank holder is at the initial position (Fig. 2b). An edge detection algorithm is used to measure the movement of the workpiece edge in relation to the undeformed blank in pixels. The draw-in is then calculated in millimeters by means of a calibration function. The results confirm that the measured values of the two measuring systems are consistent with one another with an average deviation of 0.2 mm.

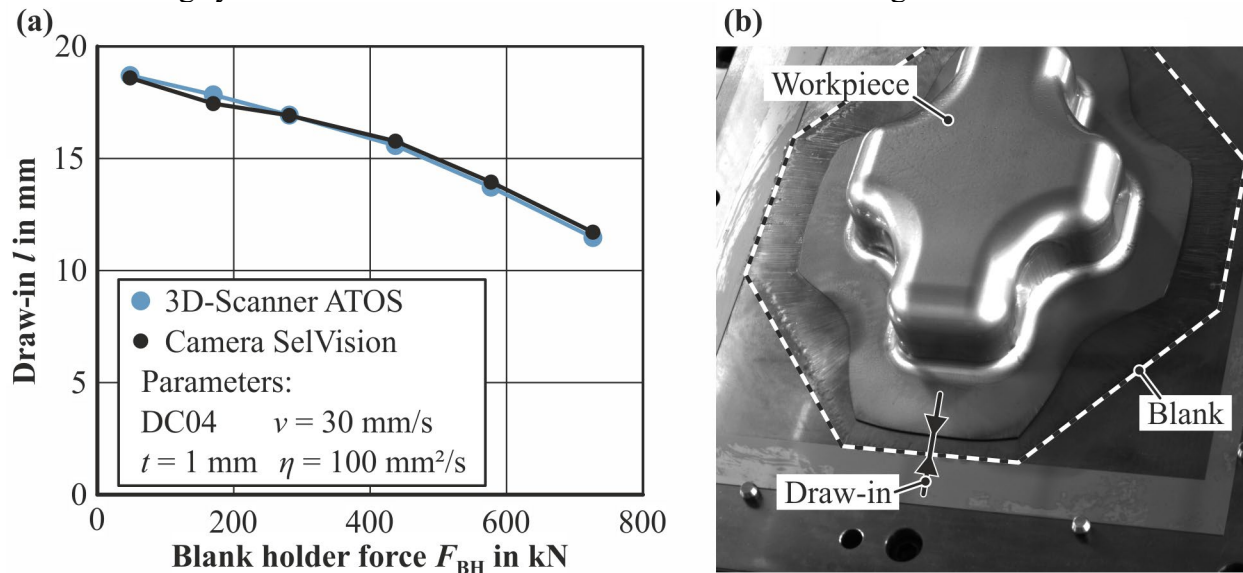


Fig. 2. (a) Comparison between ATOS and SelVision and (b) images taken by the camera

A finite element model was developed in Abaqus/explicit to investigate the influence of the coefficient of friction on the draw-in and to create a database for training the ANNs. The drawing velocity is artificially increased to minimize the computational cost, resulting in a total step time of 0.05 s. The sheet metal and tooling have been reduced to a quarter of the original size for efficient data generation. The components of the tool (e.g. punch, die, blank holder) are integrated as rigid surfaces. Friction was defined in the same way for all contacts between tool and workpiece using a constant coefficient of friction, which is varied in the following investigations. The sheet was modeled with an approximate element length of 1.5 mm and C3D8R was selected as the element type. Preliminary tests showed that a number of two elements over the sheet thickness give good agreement with the experimental results in terms of draw-in. The material properties of the four materials used in the experiments were determined by tensile tests according to DIN EN ISO 6892-1 with a gauge length of 80 mm. The properties of DC04 are discussed in more detail as this material was selected for the numerical case study. The yield curve was determined by Swift, Eq. (1), with a yield strength of  $\sigma_{F0} = 116.687$  MPa and the anisotropy was defined in accordance with Table 2. The simulation and the experiment match sufficiently well (Fig. 3a).

$$\sigma_f = 538.374 \text{ MPa} \cdot (0.004 + \varepsilon)^{0.274} \tag{1}$$

Table 2. Normal anisotropy of DC04 sheet metal with  $t = 1 \text{ mm}$

$r_0$	$r_{45}$	$r_{90}$	$\bar{r}$
2.178	1.696	2.454	2.006

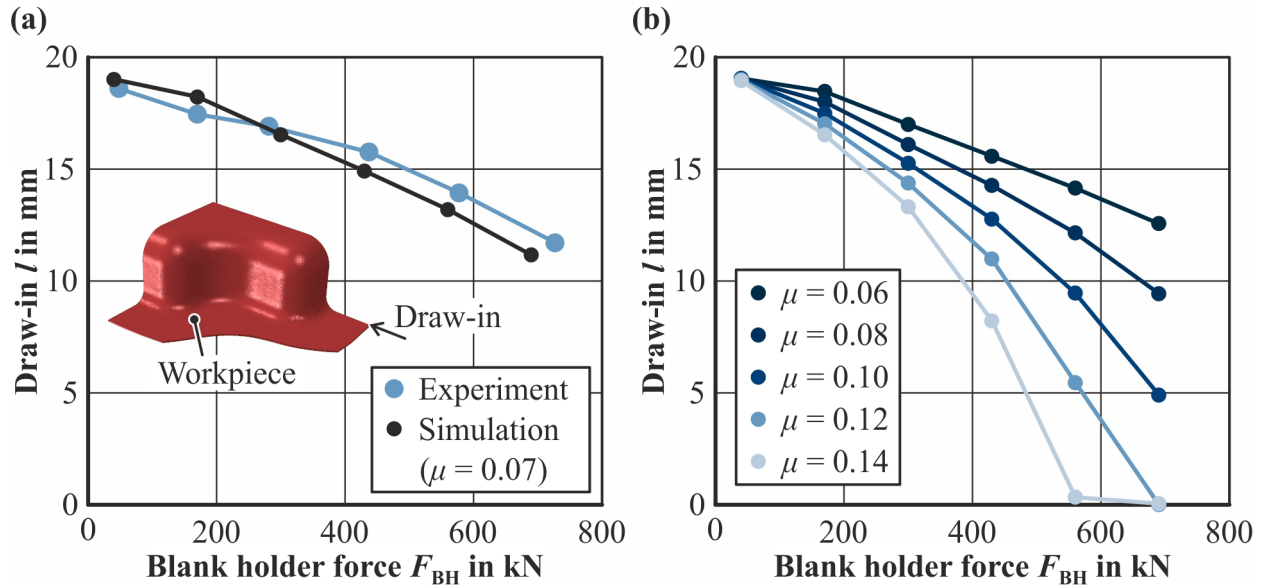


Fig. 3. (a) Comparison between simulation and experiment regarding material draw-in and (b) results of the simulation for changing coefficient of friction (DC04,  $t = 1 \text{ mm}$ )

The coefficient of friction and the BHF were varied in the simulation for each material according to Table 3. The results make it clear that the draw-in generally decreases with increasing coefficient of friction and increasing BHF (Fig 3b). For a BHF of 40 kN, the draw-in is almost identical regardless of the coefficient of friction. Since a slight wrinkling was observed in the experiments for such a low BHF, the corresponding simulation data of each material were excluded for the model training. All data where a necking was visible in the simulation and the draw-in was less than 10 mm were also excluded. In order to still have sufficient data for training the ANNs, additional simulations were then carried out for DC04 with  $t = 1 \text{ mm}$ , varying the BHF in smaller increments of 26 kN over a range of 170 kN to 690 kN for the entire range of the coefficient of friction. Ultimately, a numerical dataset with six features and 247 instances was generated.

Table 3. Parameters for the deep drawing simulations

Parameter	Value
Blank holder force $F_{BH}$ [kN]	40 – 170 – 300 – 430 – 560 – 690
Coefficient of friction $\mu$ [1]	0.06 – 0.07 – 0.08 – ... – 0.13 – 0.14 – 0.15

### Control and modelling approach

A discrete control concept has been developed that intervenes in the deep drawing process between two strokes (Fig. 4). As the material draw-in is a suitable monitoring variable, the control is designed to incorporate a camera system for draw-in detection. The target value of the draw-in is referred to as  $l_t$  and the actual measured value is referred to as  $l_a$ . The draw-in is stabilized by adjusting the BHF  $F_{BH}$ , which is determined for each stroke via PSO. The PSO implementation was realized through the open-source Python package “*pyswarm*”, where an objective function is designed to optimize  $F_{BH}$  by minimizing the absolute difference between the measured draw-in  $l_a$  and the target  $l_t$ . The algorithm iteratively updates the position of each particle in the bounded

search space based on the particle’s status and the status of the entire swarm and converges when one of the stopping criteria is met: either through reaching the maximum number of iterations permitted or through a function change smaller than the defined threshold. For this application, the default parameter values were used. The reader is referred to Wang et al. [24] for additional information on the optimization procedure of the PSO algorithm.

The objective function of the optimization algorithm is based on an ANN that predicts the draw-in  $l_p$  for various parameter combinations. As the input variables of the objective function include material properties such as sheet thickness  $t$ , yield strength  $\sigma_{R0}$  and anisotropy  $\bar{r}$ , it can be applied to different cases. Since the focus of this work is on friction, the coefficient of friction is estimated using an ANN-based softsensor, which requires the values of the bank holder force  $F_{BH}$  and the draw-in  $l_a$  of the last stroke to estimate the coefficient of friction for that stroke. If necessary, other measurements, such as the punch force, can be integrated and additional softsensors can be engaged to estimate the material properties. Moreover, a combination of target variables can be considered in the optimization algorithm. Both ANN-based models are feed forward neural networks trained to estimate a continuous target variable. For efficiently exploring the hyperparameter space, a two-stage approach was performed: in the first stage, optimal settings for the *number of hidden layers* and the corresponding *neurons per layer* as well as the non-linear *activation function* were investigated through a random search, where all possible combinations are shuffled and 50 of which are chosen at random to be tested. In the second stage, the *batch size* and the *learning rate* of the adam optimizer were investigated for the best performing parameters from stage 1. Early stopping was also included in the search as to account for computational efficiency. All combinations of the aforementioned parameters to be varied are shown in Table 4. For validation, a four-fold cross-validation approach was implemented to ensure robustness. The model’s performance for each hyperparameter set was quantified using the mean squared error across all validation folds, where the loss across all folds was computed and averaged for every combination. After this initial hyperparameter exploration, the best performing combinations were empirically used to train and test different models, this time using an 80/20 data split, stratified according to friction. With the aim to increase model generalizability, L1 and L2 regularization were tested but led to a degradation in performance and were thus not incorporated. A 5 % dropout for the neurons in the hidden layers in combination with early stopping was sufficient so as to prevent critical overfitting. The final models reached R2 values of 0.997 and 0.999 on the training set and reached similar performance on the holdout set of the split.

Table 4. Two-stage hyperparameter exploration combining random and grid search methods

Hyperparameter	Range
<b>Stage 1: 50 combinations of</b>	
Number of hidden layers	[1, 2, 3]
Neurons per layer	[4, 8, 16, 32, 64]
Activation function	[relu, tanh]
<b>Stage 2: 9 combinations of</b>	
Learning rate	[1e-2, 1e-3, 1e-4]
Batch size	[8, 16, 32]

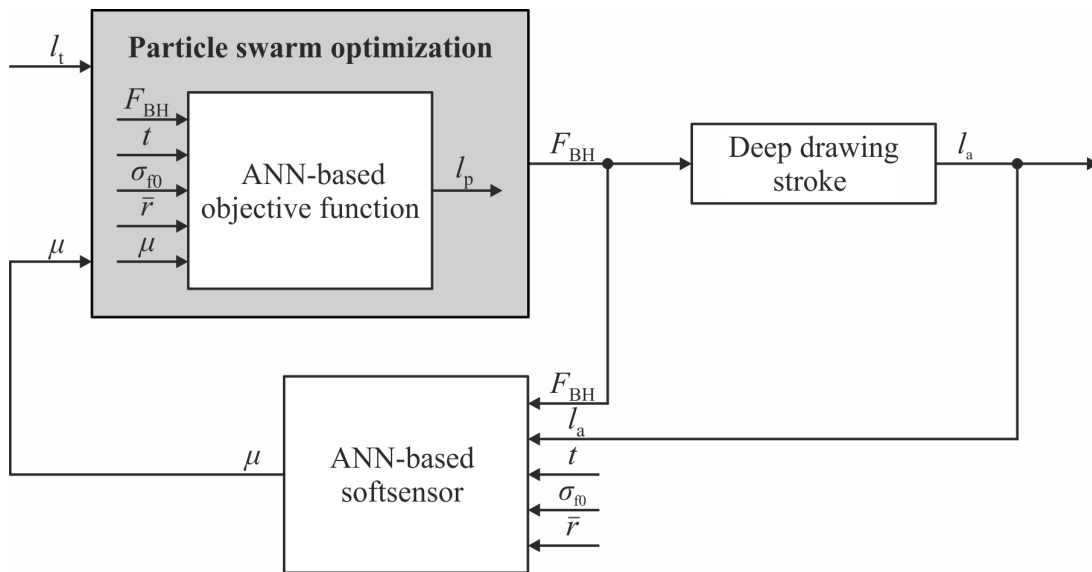


Fig. 4. Control concept with ANN-based optimization algorithm and ANN-based softsensor

**Numerical case study**

Using the simulation model described before, a case study was developed to test the functionality of the control concept and evaluate it against the uncontrolled process. For the material DC04 with a thickness of 1 mm, 25 parts with a draw-in of 16 mm are to be produced. The coefficient of friction varies between 0.07 and 0.09 and is changed arbitrarily after five parts to simulate a disturbance. In the uncontrolled process, a hold-down force of 300 kN is selected for all strokes. Initially, the draw-in is close to the target value, but larger deviations occur during the course of the case study, which illustrate the negative influence of the disturbances (Fig. 5). When using the control concept, however, the softsensor reacts to the changes of the coefficient of friction. The BHF of the first stroke is set to 300 kN. It takes one stroke for the coefficient of friction to be estimated. The optimization algorithm then adjusts the BHF so that the target value is met (Fig. 6). The fluctuation of the coefficient of friction is the same as in the uncontrolled process. Besides this disturbance, the control can deal with abrupt changes of the target value  $l_t$  from 16 to 15 mm. Overall, the case study proves that the concept is suitable for stabilizing the deep drawing process.

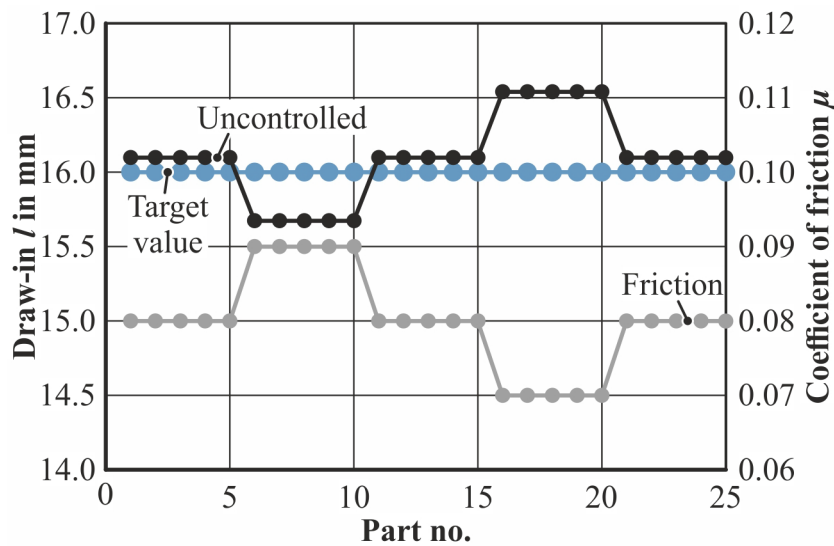


Fig. 5. Fluctuating coefficient of friction in the uncontrolled process (DC04,  $t = 1$  mm)

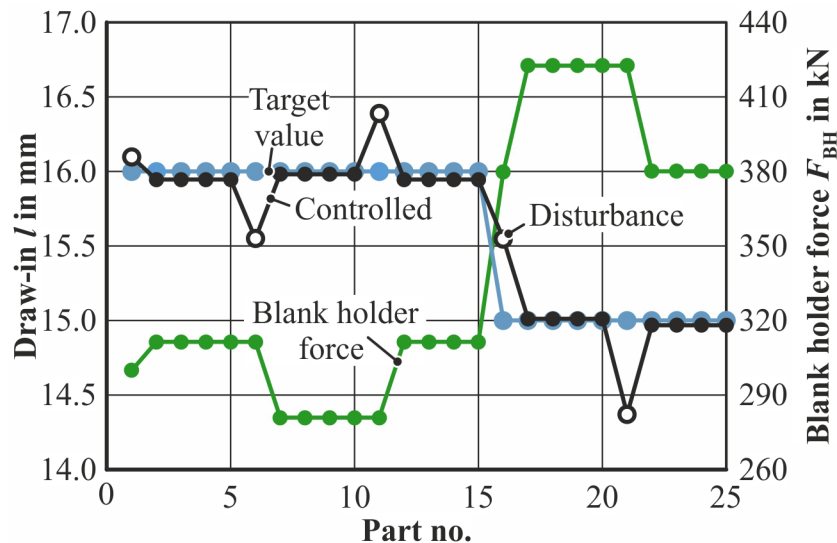


Fig. 6. Compensation of friction by adjusting the BHF (DC04,  $t = 1 \text{ mm}$ )

### Summary

The presented approach, combining real-time monitoring, predictive modeling via ANNs and optimization via PSO demonstrates the potential for significant improvements in the accuracy and stability of the sheet forming operation. The adaptability of this concept allows for the inclusion of more target variables and additional softsensors, which can act as a substitute for physical sensors. This provides a scalable solution for various types of process disturbances, while simultaneously eliminating the need for expensive and difficult to deploy measurement systems. Finally, the following conclusions can be drawn:

- Camera systems are suitable sensors for measuring the material draw-in after each stroke.
- The draw-in depends, among other things, on the blank holder force (BHF) and the lubrication conditions, such as the coefficient of friction. Since the BHF is known and the draw-in can be measured, the coefficient of friction can be estimated.
- A numerical case study proves that with this approach, the fluctuations of the coefficient of friction are detectable and can be compensated by a prediction of the optimal BHF.

### Acknowledgements

The authors kindly thank the European Regional Development Fund (EFRE) and the state of Lower Saxony for financing the research project OptimUm.

### References

- [1] B. Endelt, J. Danckert, Iterative Learning and Feedback Control Applied on a Deep Drawing Process, *Int. J. Mater. Form.* 3 (2010) 25–28. <https://doi.org/10.1007/s12289-010-0698-z>
- [2] J. Heingärtner, D. Bonfanti, D. Harsch, F. Dietrich, P. Hora, Implementation of a tribology-based process control system for deep drawing processes, *IOP Conf. Ser.: Mater. Sci. Eng.* 418 (2018) 12112. <https://doi.org/10.1088/1757-899X/418/1/012112>
- [3] J.M. Allwood, S.R. Duncan, J. Cao, P. Groche, G. Hirt, B. Kinsey, T. Kuboki, M. Liewald, A. Sterzing, A.E. Tekkaya, Closed-loop control of product properties in metal forming, *CIRP Annals.* 65 (2016) 573–596. <https://doi.org/10.1016/j.cirp.2016.06.002>
- [4] S.-W. Lo, T.-C. Yang, Closed-loop control of the blank holding force in sheet metal forming with a new embedded-type displacement sensor, *Int. J. Adv. Manuf. Technol.* 24 (2004) 553–559. <https://doi.org/10.1007/s00170-003-1711-1>



- [5] K. Siegert, M. Ziegler, S. Wagner, Closed loop control of the friction force. Deep drawing process, *J. Mater. Proc. Technol.* 71 (1997) 126–133. [https://doi.org/10.1016/S0924-0136\(97\)00158-1](https://doi.org/10.1016/S0924-0136(97)00158-1)
- [6] M. Traversin, R. Kergen, Closed-loop control of the blank-holder force in deep-drawing: finite-element modeling of its effects and advantages, *J. Mater. Proc. Technol.* 50 (1995) 306–317. [https://doi.org/10.1016/0924-0136\(94\)01389-1](https://doi.org/10.1016/0924-0136(94)01389-1)
- [7] B.A. Behrens, J.W. Yun, M. Milch, Closed-Loop-Control of the Material Flow in the Deep Drawing Process, *AMR.* 6-8 (2005) 321–328. <https://doi.org/10.4028/www.scientific.net/AMR.6-8.321>
- [8] F. Gayubo, J.L. Gonzalez, E. de La Fuente, F. Miguel, J.R. Peran, On-line machine vision system for detect split defects in sheet-metal forming processes, in: 18th International Conference on Pattern Recognition (ICPR'06), IEEE, 2006, pp. 723–726. <https://doi.org/10.1109/ICPR.2006.902>
- [9] J. Heger, G. Desai, M.Z. El Abdine, Anomaly detection in formed sheet metals using convolutional autoencoders, *Procedia CIRP.* 93 (2020) 1281–1285. <https://doi.org/10.1016/j.procir.2020.04.106>
- [10] M. Kraft, U. Bürgel, Novel concept for measurement of global blank draw-in when deep drawing outer skin automotive components, *J. Phys.: Conf. Ser.* 896 (2017) 12034. <https://doi.org/10.1088/1742-6596/896/1/012034>
- [11] S. Maier, T. Schmerbeck, A. Liebig, T. Kautz, W. Volk, Potentials for the use of tool-integrated in-line data acquisition systems in press shops, *J. Phys.: Conf. Ser.* 896 (2017) 12033. <https://doi.org/10.1088/1742-6596/896/1/012033>
- [12] S. Maier, Inline-Qualitätsprüfung im Presswerk durch intelligente Nachfolgewerkzeuge, Dissertation, Technical University of Munich, TUM.University Press, München, 2018.
- [13] A. Pierer, T. Wiener, L. Gjakova, J. Koziorek, Zero-error-production through inline-quality control of presshardened automotive parts by multi-camera systems, *IOP Conf. Ser.: Mater. Sci. Eng.* 1157 (2021) 12074. <https://doi.org/10.1088/1757-899X/1157/1/012074>
- [14] P. Fischer, J. Heingärtner, Y. Renkci, P. Hora, Experiences with inline feedback control and data acquisition in deep drawing, *Proc. Manuf.* 15 (2018) 949–954. <https://doi.org/10.1016/j.promfg.2018.07.401>
- [15] P. Fischer, J. Heingärtner, S. Duncan, P. Hora, On part-to-part feedback optimal control in deep drawing, *J. Manuf. Process.* 50 (2020) 403–411. <https://doi.org/10.1016/j.jmapro.2019.10.019>
- [16] W. Homberg, B. Arian, V. Arne, T. Borgert, A. Brosius, P. Groche, C. Hartmann, L. Kersting, R. Laue, J. Martschin, T. Meurer, D. Spies, A.E. Tekkaya, A. Trächtler, W. Volk, F. Wendler, M. Wrobel, Softsensors: key component of property control in forming technology, *Prod. Eng. Res. Devel.* (2023). <https://doi.org/10.1007/s11740-023-01227-1>
- [17] J. Zhao, F. Wang, Parameter identification by neural network for intelligent deep drawing of axisymmetric workpieces, *J. Mater. Proc. Technol.* 166 (2005) 387–391. <https://doi.org/10.1016/j.jmatprotec.2004.08.020>
- [18] K. Manabe, M. Yang, S. Yoshihara, Artificial intelligence identification of process parameters and adaptive control system for deep-drawing process, *J. Mater. Proc. Technol.* 80-81 (1998) 421–426. [https://doi.org/10.1016/S0924-0136\(98\)00121-6](https://doi.org/10.1016/S0924-0136(98)00121-6)

- [19] H. Hoffmann, M.F. Zäh, I. Faass, R. Mork, M. Golle, B. Griesbach, M. Kerschner, Automatic Process Control in Press Shops, *KEM.* 344 (2007) 881–888. <https://doi.org/10.4028/www.scientific.net/KEM.344.881>
- [20] R. Mork, Qualitätsbewertung und -regelung für die Fertigung von Karosserieteilen in Presswerken auf Basis Neuronaler Netze, Dissertation, Technical University of Munich, Herbert Utz Verlag, München, 2012.
- [21] C.C. Tai, J.C. Lin, The optimisation deep-draw clearance design for deep-draw dies, *Int. J. Adv. Manuf. Technol.* 14 (1998) 390–398. <https://doi.org/10.1007/BF01304617>
- [22] M. Manoochehri, F. Kolahan, Integration of artificial neural network and simulated annealing algorithm to optimize deep drawing process, *Int. J. Adv. Manuf. Technol.* 73 (2014) 241–249. <https://doi.org/10.1007/s00170-014-5788-5>
- [23] I. El Mrabti, A. Touache, A. El Hakimi, A. Chamat, Springback optimization of deep drawing process based on FEM-ANN-PSO strategy, *Struct. Multidisc. Optim.* 64 (2021) 321–333. <https://doi.org/10.1007/s00158-021-02861-y>
- [24] D. Wang, D. Tan, L. Liu, Particle swarm optimization algorithm: an overview, *Soft Comput.* 22 (2018) 387–408. <https://doi.org/10.1007/s00500-016-2474-6>